Original Research

Mechanisms of miR-326-5p/LCN2 signaling axis in cerebral ischemia pre-adaptation and post-adaptation to improve neuronal apoptosis

Hong Ye[1], Yu Ding*[2], Zhihong Yang[1], Lan Liu[1], Hairong Hua[1], Zhihao Mu[1]

Abstract

Post-ischemic adaptation and pre-adaptation have been recognized as effective neuroprotective tools, but the mechanism is not clear. In this paper, through the preliminary experiments, it was found that autonomous running wheel pre-adaptation could promote post-ischemic adaptation and effectively inhibit neuronal apoptosis induced by cerebral ischemia/reperfusion in mice. After high-throughput screening and luciferase experiments, the article confirmed that miR-326-5p/LCN2 signaling axis mediated the protection of neuronal damage under ischemia-reperfusion conditions by the above two means. In this project, this article intends to investigate in detail the specific molecular mechanisms and signaling pathways of miR-326-5p/LCN2 signaling axis for neuroprotection under post-adaptive and pre-adaptive binding conditions by immunoprecipitation, immunohistochemistry, database screening, apoptosis assay, and other technological means. Combined with in vivo animal experiments and isolated cell experiments, we verified the mechanism of miR-326-5p/LCN2 signaling axis and its downstream effector molecules in the process of post-adaptation and pre-adaptation to ameliorate neuronal apoptosis. This study is expected to provide new theoretical support for the protective mechanism of pre-adaptation and post-adaptation on brain tissue during ischemia. At the same time, it will provide a new theoretical basis for clinical understanding of the pathogenesis of cerebral ischemia and the development of diagnostic and therapeutic strategies.

Keywords: miR-326-5p, LCN2, Apoptosis, ischemia-reperfusion (IR)

1. Kunming Medical University
2. The Second Affiliated Hospital of Kunming Medical University

*Correspondence:719916772@qq.com

Introduction

Stroke, also known as “stroke” and “cerebrovascular accident”, is an acute cerebrovascular disease, a group of diseases caused by brain damage, including ischemic stroke and hemorrhagic stroke, which are caused by the blockage of blood vessels leading to poor blood flow to the brain, or rupture of blood vessels in the brain, triggered by a group of diseases(1). Hemorrhagic stroke, Worldwide, the mortality rate of stroke has decreased dramatically, but the burden on society and families after stroke has increased dramatically over the past 25 years due to the increase in population size and population aging(2). Currently, one person suffers a stroke every 12 seconds and one person dies of stroke every 21 seconds in our country. Revascularization is one of the effective treatments for ischemic stroke, however, some patients' symptoms worsen after revascularization in clinical practice(3). It has been found that during the treatment of ischemic diseases such as myocardial infarction or stroke, tissue damage is aggravated by the presence of excess oxygen radicals when blood flow is re-supplied, a phenomenon known as “tissue ischemia-reperfusion injury”(4). The initial stage of cerebral ischemia/reperfusion injury is vascular obstruction that causes ischemia and hypoxia in brain cells, which leads to irreversible damage to brain tissues. After subsequent recanalization of blood vessels or thrombus autolysis, an inflammatory cascade occurs in localized ischemic areas due to recanalization, which leads to increased damage to neuronal cells, and is accompanied by a decrease in the secretion of neurotrophic factors. The whole process is complicated in terms of time and space(4). It is manifested in different types, such as complete/incomplete, focal/whole-brain, transient/permanent, transient/permanent and other different types. Thrombolysis is one of the effective treatments for ischemic stroke, however, the damage caused by ischemia-reperfusion after revascularization has restricted the development of arteriovenous thrombolysis in the clinic(5).In cerebral ischemia/reperfusion injury, neuronal damage is mainly caused by intracellular imbalance of homeostasis including calcium ions, excitotoxicity, and oxidative stress, which results in irreversible neuronal damage or even neuronal death, which manifests itself in the form of neuronal cell necrosis or apoptosis(6). Generally, neuronal cells show necrosis in the central necrotic region of severe ischemia and apoptosis in the ischemic semi-dark zone. As the goal of clinical treatment, how can we greatly rescue the apoptosis of neuronal cells in the ischemic semi-dark band is a potential target for clinical treatment(7). In the process of apoptosis, the initiation and execution phases are complex and poorly understood due to the long process and the involvement of a large number of apoptosis-related signaling pathways/molecules, making them a hot and difficult topic for clinical and scientific research. It is currently recognized that apoptosis consists of two pathways, the exogenous apoptosis pathway and the endogenous apoptosis pathway. The exogenous pathway is the binding of Fasl ligand, a member of the tumor necrosis factor superfamily, to the Fas receptor located on the surface of the neuronal cell membrane, which causes a conformational change of Fas itself, which then binds to its related death domain protein FADD and activates Caspase-8(8). The endogenous pathway refers to the mitochondrial apoptosis pathway, i.e., in the presence of a lack of growth factors, DNA damage, etc., the mitochondrial membrane depolarizes, the membrane potential decreases, and the mitochondrial apoptosis pathway is activated. Membrane potential decreases, the mitochondrial transition pore opens, and a large number of apoptosis-related proteins inside the mitochondria, such as apoptosis-inducing factor AIF(9), cysteine asparaginase, nucleic acid endonuclease G,

cytochrome C, and PROCASPASE2-3-8-9 are released in large quantities, resulting in the programmed death of cells. On the one hand, in the presence of dATP/ATP, Cyt C and proaspase-9 can merge with apoptosis-activating factor-1 to form apoptotic bodies, which activate Caspase-9 and then activate the downstream Caspase-3, causing apoptosis(10). On the other hand, external factors such as cell ischemia and hypoxia can promote, and induce the initiation of regulation.

Materials and Methods

Exercise pre-adaptation and post-adaptation animal models and grouping

C57BL6 mice, SPF grade, male, 4-4.5 weeks old, weighing 18.52±0.63 g, were provided by the Department of Laboratory Animal Science, Kunming Medical University. Single-cage rearing, 1 mouse/cage, counting 65 mice. Feeding methods and conditions: free-feeding and drinking water, fed with national standard rodent dry feed, indoor temperature of 22±1 degrees Celsius, humidity maintained at 40%-60%, and natural day and night alternating light.

Autonomous running wheel exercise as a model of exercise pre-adaptation, in order to avoid the interference caused by the experimental grouping, so in the pre-grouping need to select mice with basically the same motor ability into the group for observation, in order to prevent the emergence of the quiet group contains mice with strong motor ability and active mice, while the exercise group contains mice with poor motor ability and quiet mice, which affects the subsequent experimental development and statistics. Specific screening methods: prepare cages with running wheels, place each mouse in the cage, observe and record the number of laps, eliminate mice with too many or too few laps, and take 50 mice with a similar number of laps to be included in the group for experimental observation.

Volumetric determination of cerebral infarct foci

2,3,5- Triphenyl-2 H-tetrazolium chloride (TTC), a fat-soluble complex originally used to assay seed viability, is a proton receptor for the pyridine mononucleoside structuring enzyme system in the respiratory chain and is characterized by photosensitivity. It was used in the 1950s for the detection of ischemic infarction in tissues. Normal tissue using TTC reacts with dehydrogenase and is reduced to a red color, whereas in ischemic tissue, where dehydrogenase activity is decreased or lost, there is not enough to react and it appears pale.

In situ detection of apoptosis by immunohistochemistry and TUNEL assay

Principle of TUNEL assay: When apoptosis occurs, DNA breaks occur, and these DNA breaks can be recognized by enzyme-labeled nucleotide 3'OH-free ends. The dUTP labeled with fluorescein can be transferred to the 3' end of the DNA fragment under the action of terminal deoxynucleotidyl transferase (TdT) to label the DNA strand break end nick. At the same time, the fluorescein can be recognized by the Fab segment antibody, and due to the binding of horseradish peroxide, it can be specifically colored to locate the apoptotic cells after the addition of the enzyme substrate DAB, which can be detected by ordinary light microscopy.

Extraction of RNA from tissue blocks and cells

Total RNA was extracted from tissue blocks or cells by one-step extraction with Trizol, concentrated by isopropanol precipitation, and quantified by photometer and formaldehyde denaturing gel electrophoresis. miRNA isolation, 50-100.0 μg of total RNA was used to isolate miRNA by Ambion's miRNA Isolation Kit (Cat# 1560) or the polyethylene glycol method (FEBS Letters, 2005, 579:318-324). Fluorescent labeling of miRNA samples Li Fluorescent labeling with T4 RNA ligase labeling method, followed by precipitation with anhydrous ethanol, blow-drying and use for microarray hybridization.

Western Blot assay

After execution of mice by the guillotine method the skull was opened using bone forceps and the brain tissue was removed The brain tissue was quickly washed using pre-cooled 0.1 M PBS to remove tissue fluid and blood. 80-100 mg of brain tissue was added to the lysate and homogenized manually in an ice bath for 2 minutes. The individual tissue specimens were then centrifuged after the addition of buffer 0.5 m1 and PMSF 5 μl 10 mg/mI with the parameters of 4° C, 12,000 g/min for 40 min. After centrifugation, the supernatant was transferred into tubes dispensed in 0.5 ml using a pipette and stored in a refrigerator at -80° C. The total amount of proteins in the samples was determined using the BCA method, and then the total amount of proteins in each group was calculated and quantified to be 50ug for subsequent electrophoresis experiments. The data were obtained by taking photographs after immunostaining.

Immunoprecipitation

Collect the harvested cells 24-48 h after simultaneous transfection, add appropriate amount of cell lysis buffer (containing protease inhibitors), lysed on ice for 30 min, centrifuged the cell lysate at 4° C for 30 min at maximum speed, and then extracted the supernatant; a small amount of the lysate was prepared for Western blot analysis, and 1 μg of the remaining lysate plus 1 μg of the corresponding antibody was added to the cell lysate, and incubated overnight at 4° C with slow shaking. Incubate overnight; take 10ul of protein A agarose beads, wash 3 times with appropriate amount of lysis buffer, and centrifuge at 3,000 rpm for 3 min each time; add 10 μl of the pretreated protein A agarose beads into the cell lysate incubated with the antibody overnight and incubate at 4° C with slow shaking for 2-4h, so as to make the antibody couple with the protein A agarose beads; after immunoprecipitation, incubate at 4° C at 3° C for 3 hours to make the antibody couple with the protein A agarose beads; after immunoprecipitation, incubate at 4° C at 4° C at 3 hours to make the antibody and the protein A agarose beads couple. After the immunoprecipitation reaction, the agarose beads were centrifuged to the bottom of the tube at 3,000 rpm for 3 min at 4° C; the supernatant was carefully aspirated, and the agarose beads were washed 3-4 times with 1 ml of lysis buffer; finally, 15 μl of 2× SDS sample buffer was added, and the sample was boiled for 5 min; the sample was then analyzed by SDS-PAGE, Western blotting or mass spectrometry. Analysis. The binding protein was determined by immunoprecipitation.

Statistical analysis

Statistical analysis was performed using the SPSS 17.0 software (SPSS, Chicago, USA). Data were expressed as mean ± standard deviation (SD). Three replicates were included in each independent experiment. Student's t-test and ANOVA were used for statistical analysis. Statistical significance was regarded as $P<0.05$.

Results

Inhibition of miR-326-5p expression enhances the ameliorative effect of IP in IR mice, and recovery is better in the case of co-intervention of IP and RW

The group chose C57BL6 mice, autonomous running wheel exercise as a model of exercise pre-adaptation, and anesthetized mice with pentobarbital injection intraperitoneally to establish a mouse IR model. The expression of miR-326-5p was detected by qPCR. Compared with the sham group, miR-326-5p expression was increased in the IR group, relatively decreased after intervention by IP, and decreased again after injection of sh-miR-326-5p. miR-326-5p expression was decreased in the group using co-intervention of IR and RW, and decreased after transfection of sh-miR-326-5p, both groups. 5p expression was reduced after transfection with sh-miR-326-5p, and the expression level in these two groups was overall less than that in the group intervened with IP alone, as shown in Fig. 1A. After the model was established, the mice in each group were executed by cervical dislocation method, and the volume of cerebral infarct foci was measured by the method of TTC assessment; no infarcts were seen in the sham group, and the rest of the groups had different degrees of cerebral swelling and definite infarct foci formation in the ischemic side of the mice, and the normal cerebral tissues stained by TTC appeared red, and the infarcts TTC staining of normal brain tissue was red, and the infarct foci were pale white. After injection of sh-miR-326-5p, the volume of mouse infarct foci was reduced in the groups of IP intervention alone and IP, RW co-intervention, and the reduction of co-intervention was greater than that of the group of intervention alone, Fig. 1B. The loss of neurons in mice after IR was observed by immunohistochemistry staining, and the number of neurons was observed and counted by staining, comparing with that of the sham group, the number of positive neuronal cells was smaller in IR group, and the number of positive neuronal cells was lower in TTC-stained normal brain tissues by IP alone and sham group. The number of positive neuronal cells was lower in the IR group, and increased after co-intervention of IP alone and IP, RW, and after knockdown of miR-326-5p, the number of neuronal cells was increased, and the extent of the increase was larger in the co-intervention group, Fig. 1C. By observing the morphology of the neurons in each group, it was found that neuronal synaptic lengths were shortened in the IR group and increased after co-intervention of IP alone and IP, RW, and knockdown of miR-326-5p, and the extent of the increase was greater in the co-intervention group, Fig. 1C. The neuronal synapse length increased

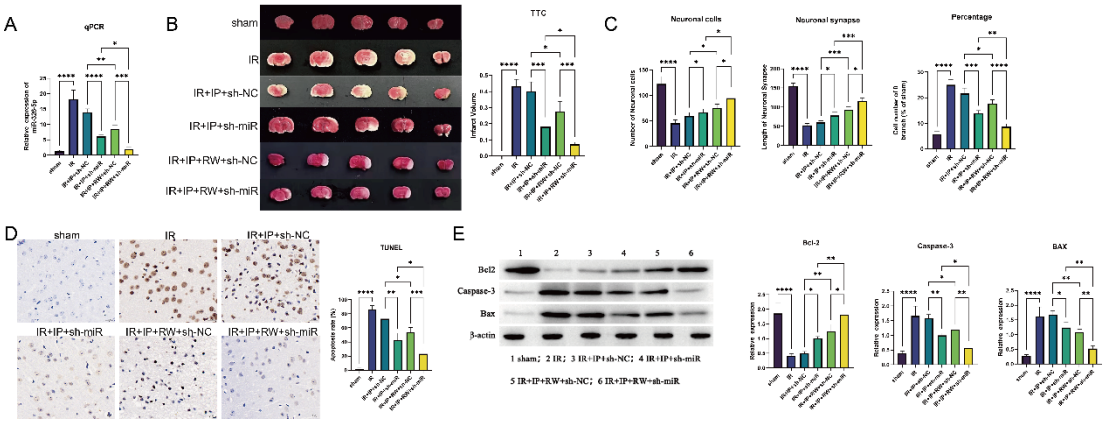

Figure 1 The effect of miR-326-5p on IR.

(A) Detection of miR-326-5p expression by qpcr. B) Detection of the volume of cerebral infarct foci in mice by TTC. C) Number of neuronal cells, length of synapses, proportion of axon terminals without branches. D) TUNEL staining for detection of neuronal apoptosis. E) Western blot detection of apoptosis-related protein expression **P*<0.05, ***P*<0.01, ****P*<0.001.

after knockdown of miR-326-5p, and the extent of increase was larger in the co-intervention group, Figure 1C. Compared with the sham group, IR resulted in an increased proportion of branchless neurons at the axon terminals, and the proportion was reduced after co-intervention by IP alone and IP, RW, and the proportion was reduced after knockdown of miR-326-5p, and the extent of reduction was larger in the co-intervention group was larger, Figure 1C. neuronal apoptosis in ischemia-tested brain tissues of each group was examined by means of TUNEL staining. The results observed that there were fewer positive results in the sham group, while the positive cells were denser in the IR group, and the number of positive cells was reduced and distributed sporadically after co-intervention by IP alone and IP,RW, and the number of positive cells was reduced after knockdown of miR-326-5p, and the degree of its reduction was larger in the co-intervention group, as shown in Fig. 1D. Apoptosis-related proteins were detected by Western blot, and the results observed that apoptosis-repressive proteins, the results observed that the apoptosis inhibitor protein, Bcl-2, was decreased in the IR group, and the expression of Bcl-2 was decreased after co-intervention by IP alone and IP, RW, and the expression was decreased after knockdown of miR-326-5p, and the extent of its decrease was larger in the co-intervention group; the pro-apoptotic protein, Bax, and apoptotic marker, Caspase3, were increased, and the expression of knockdown of miR-326-5p was increased and its increase was greater in the co-intervention group, Figure 1E.

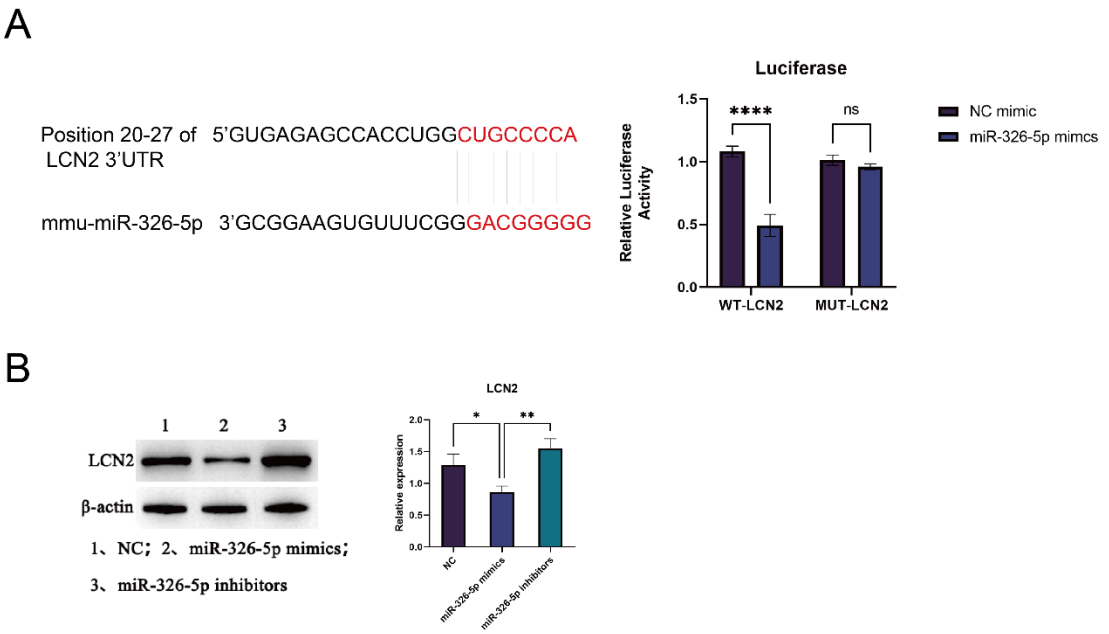

Figure 2 LCN2 is a target of miR-326-5p

A) Prediction and validation of targeting relationship between miR-326-5p and LCN2. B) Negative regulatory relationship between miR-326-5p and LCN2 $^{*}P<0.05$, $^{**}P<0.01$.

We predicted the binding targets of miR-326-5p and LCN2 by TargetScanMouse 8.0 database, and verified the targeting relationship by dual luciferase Dual luciferase assay showed that up-regulation of miR-326-5p decreased the relative luciferase activity of WT-LCN2 vector. However, there was no significant difference in the relative luciferase activity of the MUT-LCN2 plasmid, Figure 2A. The regulatory relationship between miR-326-5p and LCN2 was visualized by

Western blot, and LCN2 expression was decreased after transfection of miR-326-5p mimics, whereas after transfection of miR-326-5p inhibitor, LCN2 expression increased, illustrating the negative regulatory relationship between miR-326-5p and LCN2, Figure 2B.

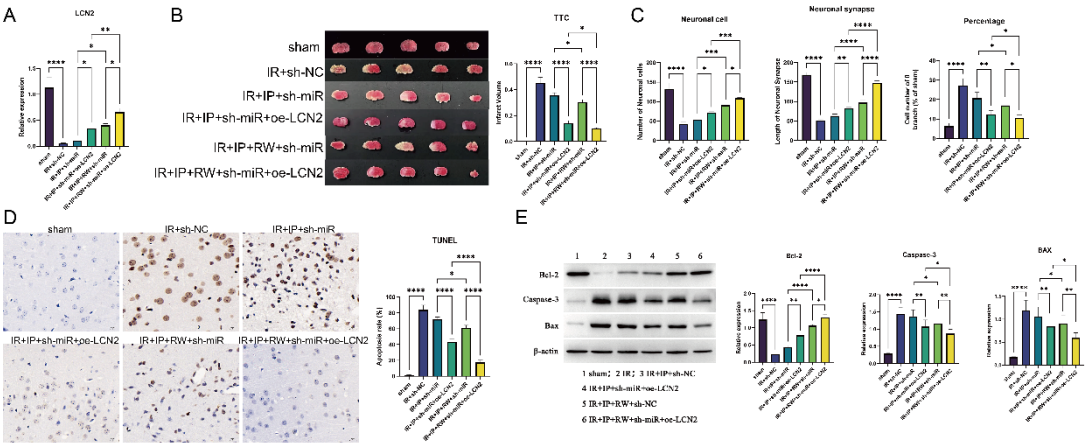

Figure 3 miR-326-5p targets LCN2 after ischemia-reperfusion injury

A) Transfection efficiency was detected by qPCR. B) Detection of the volume of cerebral infarct foci in mice by TTC. C) Number of neuronal cells counted, synapse length counted, proportion of axon terminals without branching neurons counted. D) TUNEL staining for detection of neuronal apoptosis. E) Western blot detection of apoptosis-related protein expression. $^{*}P<0.05$, $^{**}P<0.01$.

To study the role of miR-326-5p targeting LCN2 to regulate LCN2 after ischemia-reperfusion injury, we transfected oe-LCN2 into IR+IP+sh-miR and IR+IP+RW+sh-miR groups, and after transfection, we examined the expression of LCN2 to confirm the efficiency of the transfection by qPCR, and the expression of LCN2 was increased in the groups that underwent the transfection operation, and increased more in the IP and RW co-intervention groups, the increase was higher, as shown in Figure 3A.Cerebral infarct foci volume assay was assessed by the method of TTC, and all groups of IR had varying degrees of cerebral swelling and definite infarct foci formation in ischemic lateral mice. After injection of sh-miR-326-5p, the volume of cerebral infarct foci was reduced in mice in the groups of IP intervention alone and IP, RW co-intervention, and transfection of oe-LCN2 facilitated this result, and the volume of cerebral infarct foci was reduced compared with that of injection of sh-miR-326-5p, and the degree of reduction in the co-intervention was greater than that of the group of IP alone, as shown in Fig. 3B.By immunohistochemistry staining, the mouse Neuronal loss was observed and counted by staining, the number of positive neuronal cells was low in the IR group, and increased by IP alone and IP,RW co-intervention, and the number of neuronal cells was increased by knockdown of miR-326-5p, and transfection of oe-LCN2 facilitated this result, and the extent of its increase was greater in the co-intervention group, Fig. 3C.By observing the neuronal morphology in each group, it was found that neuronal synapse length was shortened in the IR group, and increased after co-intervention by IP alone and IP, RW, after knockdown of miR-326-5p, and transfection of oe-LCN2, which facilitated this result, and neuronal synapse length was increased, and the extent of its increase was greater in the co-intervention group, Figure 3C. compared with the sham group. IR resulted in an increase in the proportion of axon terminal unbranched neurons, which was reduced after co-intervention by IP alone and IP, RW, and after knockdown of miR-

326-5p, which was facilitated by transfection of oe-LCN2, and the extent of the reduction was greater in the co-intervention group, Figure 3C. Neuronal apoptosis of ischemia-tested brain tissues of the groups by TUNEL staining was were examined. It was observed that there were fewer positive results in the sham group and denser positive cells in the IR group, and after co-intervention by IP alone and IP, RW, the number of positive cells was reduced and distributed sporadically, and the number of positive cells was reduced after knockdown of miR-326-5p, which was facilitated by transfection of oe-LCN2, and the degree of its reduction was greater in the co-intervention group, as shown in Fig. 3D. Apoptosis-related proteins were detected by Western blot, and the results observed that the apoptosis-suppressing protein Bcl-2, which was decreased in the IR group, was decreased after co-intervention by IP alone and IP, RW, and increased after knockdown of miR-326-5p, and its in increase was greater in the co-intervention group; the pro-apoptotic protein Bax and apoptosis marker Caspase3 were increased and knockdown of miR-326-5p expression was increased; transfection of oe-LCN2 facilitated these results, and its increase was greater in the co-intervention group, Figure 3E.

LCN2 targets MMP2 to modulate injury after ischemia-reperfusion

In order to study the regulatory mechanism of LCN2 and its interacting proteins in IR, we screened proteins with interactions with LCN2 through STRING database (STRING: functional protein association networks (string-db.org)), and screened with apoptosis-related genes through intersection screening, and obtained MMP2 as a candidate gene for validation. MMP2 was obtained as a candidate gene for validation, and the regulatory relationship between LCN2 and MMP2 was verified by COIP, Figure 4A. In order to verify whether LCN2 regulates its pathological mechanism through MMP2 in IR, after constructing the model, oe-LCN2 and sh-MMP2 were transfected, and it was found by Western blot analysis that, after transfecting oe-LCN2, LCN2 , MMP2, and p-MMP2 expression were increased, and after transfection with sh-MMP9, these expressions were decreased, Figure 4B. To assess, the role of LCN2 and its reciprocal protein MMP2 in IR, cerebral infarct foci volume measurements were assessed by the method of TTC, and cerebral swelling and definitive infarct foci formation were found in all groups of IR in mice with varying degrees of cerebral swelling and definite infarct foci formation in the ischemic side of the ischemic side of the ischemic side of the ischemic side of the ischemic side of the ischemic side. Injection of oe-LCN2 decreased the volume of cerebral infarct foci in in mice, whereas transfection of sh-MMP2 increased the volume of cerebral infarct foci, Figure 4C.Survival of neurons in mice was observed by immunohistochemical staining, and the number of neurons was observed and counted by staining.The number of positive neuronal cells was low in the IR group, and the number of cells was increased in comparison with the IR group after transfection of oe-LCN2, whereas the number of cells was increased in the IR group after transfection of sh-MMP2 increased the number of neuronal cells, reversing this result, Figure 4D. By observing the neuronal morphology in each group, it was found that neuronal synapse length was shortened in the IR group, increased after transfection with oe-LCN2, and after transfection with oe-MMP2, reversed this result, and the neuronal synapse length was increased, Fig. 4D. Compared with the sham group, IR led to an increase in the proportion of axon terminal unbranched neurons, and after transfection with oe-LCN2, the proportion was decreased, while transfection with sh-MMP2 reversed this result and the proportion of axon terminal branchless neurons decreased, Figure 4D. Neuronal apoptosis in ischemia-tested brain tissues of each group was examined by TUNEL staining. It was observed that there were fewer

positive results in the sham group, while the positive cells were more dense in the IR group, and by transfection of oe-LCN2, the number of positive cells was reduced and the distribution was fragmented, which was reversed by transfection of sh-MMP2 with an increase in the number of positive cells, as shown in Fig. 4E. Apoptosis-related proteins were detected by Western blot, and the results observed that apoptosis suppressor protein Bcl-2, which was decreased in the IR group, was increased after transfection of oe-LCN2, while sh-MMP2 resulted in decreased expression; pro-apoptotic protein Bax and apoptotic marker Caspase3 were increased, and the expression of knockdown miR-326-5p was increased, which was reversed after transfection of oe-LCN2, as shown in Figure 4F.

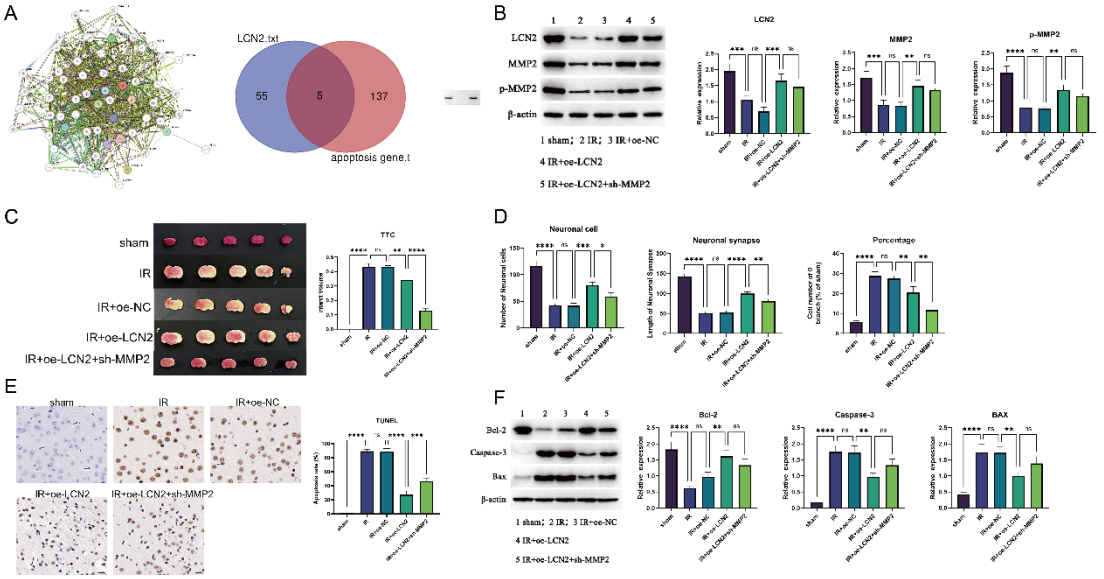

Figure 4 LCN2 targets MMP2 to modulate injury after ischemia-reperfusion.

A) Transfection efficiency was detected by qPCR. B) Detection of the volume of cerebral infarct foci in mice by TTC. C) Number of neuronal cells counted, synapse length counted, proportion of axon terminals without branching neurons counted. D) TUNEL staining for detection of neuronal apoptosis. E) Western blot detection of apoptosis-related protein expression., $^{\#}P<0.05$, $^{\#\#}P<0.01$.

compared with the NC group, overexpression of miR-192-5p significantly increased the n

Discussion

The unpredictability of cerebral ischemia limits the clinical use of ischemic preadaptation. Some studies have shown that the protective effect of post-ischemic adaptation is comparable to that of ischemic preadaptation(11). Moreover, because postadaptation is implemented after ischemia-reperfusion, it makes it better clinically actionable. Therefore, post-ischemic adaptation, i.e., a brief, repetitive process of opening and reclosing at the onset of reperfusion, followed by restoration of blood flow, may improve myocardial tolerance to ischemia(12). Using the acute myocardial infarction model in dogs, it has been demonstrated that ligation of the anterior descending branch of the left coronary artery in dogs for 1h hours, followed by three consecutive cycles of repetitive opening for 30s and reclosing for 30s, followed by restoration of coronary blood flow, can reduce the extent of infarction by 44% compared with the control group, which is the same as that of ischemic pre-adaptation group to reduce the extent of infarction(13). Since then, numerous scholars have demonstrated that post-adaptation can significantly reduce the degree of myocardial reperfusion injury and edema, improve cardiac function, inhibit reperfusion

arrhythmias, and reduce no-reflow or microvascular embolism(14). Ma et al.(15), using the rat as an animal model, found that the Nrf2-ARE pathway was activated by repeated 3-cycle reperfusion\ischemia for 5 min operation of the middle cerebral artery and the corresponding Nrf2\HOI\ NQOI expression was up-regulated, malondialdehyde was down-regulated, SOD was increased, the level of oxidative stress was decreased, the infarct volume of brain tissue was reduced, the severity of cerebral edema was reduced, neurological function was restored to a certain extent, and ischemia-reperfusion injury was reduced(16).

In order to further clarify the mechanism of exercise pre-adaptation to promote post-adaptation inhibition of apoptosis and downstream detailed signaling pathways applicants compared the expression of microRNAs under post-adaptation and ischemia-reperfusion models by miRNAs microarray screening(17). Meanwhile, RT-PCR was performed on the basis of exercise pre-adaptation, and exercise pre-adaptation reduced the expression of miR-326-5p and elevated the expression of LCN2 on the basis of post-adaptation, which attenuated neuronal apoptosis.

miRNAs are non-coding small molecule RNAs of 18-25 nucleotides in length, which are composed of hairpin-shaped single-stranded RNA precursors of 70-90 nucleotides and processed by the enzyme Dicer(18). miRNAs play their roles by binding to the mRNAs of the target genes and inhibiting the translation of the target genes or directly leading to the degradation of the target genes. In order to investigate the downstream target genes of miR-326-5p, we confirmed that LCN2 is the downstream target gene of miR-326-5p through bioinformatics analysis and luciferase assay.

After constructing a mouse IR model, miR-326-5p expression was regulated by stereotactic injection. miR-326-5p was highly expressed in IR, and the expression was similarly suppressed by post-adaptation (IP)(19). miR-326-5p expression was decreased by knockdown of miR, and miR-326-5p expression was decreased by the addition of pre-adaptation (RW); by constructing a mouse IR model After that, miR-326-5p expression was regulated by stereotactic injection, and the results indicated that miR-326-5p expression was decreased in the IP group, and after knockdown of miR-326-5p, it was found that the area of cerebral infarcted tissues was reduced, the number of surviving neuronal cells was increased, the axon length of neurons was increased, the proportion of axon terminals with no branching neurons was reduced, and apoptosis was reduced; and the addition of further RW interference LCN2 is one of the targets of miR-326-5p, and miR-326-5p and LCN2 are negatively regulated. miR-326-5p targets LCN2 to regulate the reperfusion model of cerebral ischemic injury in mice, which was demonstrated by the decrease in the area of cerebral infarcted tissues, increase in the number of living neuronal cells, increase in the length of neuronal axons, and increase in the length of neuronal axons, and decrease in cellular apoptosis after the knockdown of miR-326-5p. increased, neuronal axon length increased, the proportion of branchless neurons at axon terminals decreased, and apoptosis decreased, whereas injection of LCN2 reversed these effects; similarly, these effects were enhanced by the addition of RW measures.MMP2 and LCN2 are proteins with a reciprocal relationship, and overexpression of LCN2 decreased the area of cerebral infarcted tissue found to be decreased, increased the number of surviving neuronal cells, neuronal axon length, reduced the proportion of axon terminals without branching neurons; and reduced apoptosis; while transfection with sh-MMP2 reversed these effects.

LCN2 is a glycoprotein with a molecular weight of 25,000 and is the No. 2 member of the lipid carrier protein family(20). LCN2 plays different regulatory roles in a variety of cellular processes such as cell death, survival, migration, invasion

and iron delivery(21). LCN2 is highly upregulated when the organism is in an inflammatory state and plays a role in regulating macrophage activation in the liver and brain(22). It has been shown that neurons and glial cells in the central nervous system are cellular sources of LCN2. Especially in glial cells, LCN2 expression is up-regulated in cerebral hemorrhage, spinal cord injury, chronic inflammatory pain, and ischemic stroke, and is involved in the development of the disease. There are two types of cellular receptors for LCN2: the first one is megalin, which belongs to a multiligand endocytosis receptor and is mainly expressed by renal epithelial cells to promote renal reabsorption of LCN2(23); and the second is 24p3r, which belongs to the organic cation transporter family and is expressed by renal epithelial cells to promote renal LCN2 reabsorption(24). cation transporter family, which is expressed in many tissues and present at particularly high levels in renal epithelial cells, macrophages, neutrophils, microglia, astrocytes and neurons. In LPS-induced inflammation models, LPS induces the secretion of LCN2 from the central nervous system as a co-signal to activate astrocytes and microglia and promote neurovascular repair after stroke and brain injury(25).

Effects of miR-326-5p expression after cerebral ischemia-reperfusion injury and its interventions (pre-adaptation, post-adaptation); Role of miR-326-5p expression on functional recovery of neurons after IR in mice; Targeting relationship between miR-326-5p and LCN2; Involvement of miR-326-5p in the functional modulation of neurons after IR in mice by targeting LCN2; Prediction of LCN2 downstream target genes as well as screening; LCN2 is involved in the functional regulation of neurons after IR in mice by targeting MMP2 regulation.

The present study mainly evaluates the functional recovery of neurons after IR injury through pre-adaptation and post-adaptation as well as the regulation of molecular axes expression. In order to closely correlate the results with the clinical reagents, in-depth correlation studies will be carried out with the clinical observation indexes, such as neuroimaging, Neurocognitive Function Measurement Scale (NFMS) data, and the patients' long-term follow up data, etc., so that the clinical significance of biomolecule axes will be sought for the diagnosis and treatment of IR. We will also conduct in-depth correlation studies with clinical indicators such as neuroimaging data and patients' long-term follow-up data, in order to seek for clinically meaningful biomolecular axes for IR diagnosis and treatment.

References

1. Litman M, Martin K, Spratt NJ, Beard DJ. Quantification of Leptomeningeal Collateral Blood Flow in Hypertensive Rats during Ischemic Stroke. Journal of stroke and cerebrovascular diseases : the official journal of National Stroke Association. 2024:108195.
2. Oloko-Oba M, Liu Y, Wood K, Lloyd MS, Ho JC, Hertzberg VS. Machine Learning-Based Identification of High-Risk Patterns in Atrial Fibrillation Ablation Outcomes. medRxiv : the preprint server for health sciences. 2024.
3. Bullock-Palmer RP, Einstein AJ, Srichai MB. How cardiac computed tomography angiography and positron emission tomography play complementary roles in a Practice's business model. Journal of cardiovascular computed tomography. 2024.
4. Zhu S, Pan W, Yao Y, Shi K. The efficacy of colchicine compared to placebo for preventing ischemic stroke among individuals with established atherosclerotic cardiovascular diseases: a systematic review and meta-analysis. Scandinavian cardiovascular journal : SCJ. 2024:1-11.
5. Lin G, Jiang P, Lou M. Thrombolysis in Ischemic

Stroke Patients with Isolate Pulmonary Arteriovenous Malformations. Journal of stroke and cerebrovascular diseases : the official journal of National Stroke Association. 2019;28(6):e68-e70.

6. Jomova K, Makova M, Alomar SY, Alwasel SH, Nepovimova E, Kuca K, et al. Essential metals in health and disease. Chemico-biological interactions. 2022;367:110173.
7. Fricker M, Tolkovsky AM, Borutaite V, Coleman M, Brown GC. Neuronal Cell Death. Physiological reviews. 2018;98(2):813-80.
8. Song C, Liu D, Liu S, Li D, Horecny I, Zhang X, et al. SHR1032, a novel STING agonist, stimulates anti-tumor immunity and directly induces AML apoptosis. Sci Rep. 2022;12(1):8579.
9. Xue Q, Kang R, Klionsky DJ, Tang D, Liu J, Chen X. Copper metabolism in cell death and autophagy. Autophagy. 2023;19(8):2175-95.
10. Xi C, Wu J. dATP/ATP, a multifunctional nucleotide, stimulates bacterial cell lysis, extracellular DNA release and biofilm development. PloS one. 2010;5(10):e13355.
11. Wang M, Pan W, Xu Y, Zhang J, Wan J, Jiang H. Microglia-Mediated Neuroinflammation: A Potential Target for the Treatment of Cardiovascular Diseases. Journal of inflammation research. 2022;15:3083-94.
12. Messadi E, Vincent MP, Griol-Charhbili V, Mandet C, Colucci J, Krege JH, et al. Genetically determined angiotensin converting enzyme level and myocardial tolerance to ischemia. FASEB journal : official publication of the Federation of American Societies for Experimental Biology. 2010;24(12):4691-700.
13. Tiryakioğlu M, Aliyu MN. Myocardial bridge. Folia morphologica. 2020;79(2):411-4.
14. Yasmin F, Najeeb H, Naeem U, Moeed A, Atif AR, Asghar MS, et al. Adverse events following COVID-19 mRNA vaccines: A systematic review of cardiovascular complication, thrombosis, and thrombocytopenia. Immunity, inflammation and disease. 2023;11(3):e807.
15. Ma Z, Ma Y, Cao X, Zhang Y, Song T. Avenanthramide-C Activates Nrf2/ARE Pathway and Inhibiting Ferroptosis Pathway to Improve Cognitive Dysfunction in Aging Rats. Neurochemical research. 2023;48(2):393-403.
16. He F, Ru X, Wen T. NRF2, a Transcription Factor for Stress Response and Beyond. Int J Mol Sci. 2020;21(13).
17. Gao L, Qiu F, Cao H, Li H, Dai G, Ma T, et al. Therapeutic delivery of microRNA-125a-5p oligonucleotides improves recovery from myocardial ischemia/reperfusion injury in mice and swine. Theranostics. 2023;13(2):685-703.
18. Plotkin LI, Wallace JM. MicroRNAs and osteocytes. Bone. 2021;150:115994.
19. Yao Q, Chen Y, Zhou X. The roles of microRNAs in epigenetic regulation. Current opinion in chemical biology. 2019;51:11-7.
20. Jaberi SA, Cohen A, D'Souza C, Abdulrazzaq YM, Ojha S, Bastaki S, et al. Lipocalin-2: Structure, function, distribution and role in metabolic disorders. Biomedicine & pharmacotherapy = Biomedecine & pharmacotherapie. 2021;142:112002.
21. Lee S, Jha MK, Suk K. Lipocalin-2 in the Inflammatory Activation of Brain Astrocytes. Critical reviews in immunology. 2015;35(1):77-84.
22. Yan L, Yang F, Wang Y, Shi L, Wang M, Yang D, et al. Stress increases hepatic release of lipocalin 2 which contributes to anxiety-like behavior in mice. Nature communications. 2024;15(1):3034.
23. Hakim O, John S, Ling JQ, Biddie SC, Hoffman AR, Hager GL. Glucocorticoid receptor activation of the Ciz1-Lcn2 locus by long range interactions. The Journal of biological chemistry. 2009;284(10):6048-52.
24. Li J, Xu P, Hong Y, Xie Y, Peng M, Sun R, et al. Lipocalin-2-mediated astrocyte pyroptosis promotes neuroinflammatory injury via NLRP3 inflammasome activation in cerebral ischemia/reperfusion injury. Journal of neuroinflammation. 2023;20(1):148.
25. Gong F, Li R, Zheng X, Chen W, Zheng Y, Yang

Z, et al. OLFM4 Regulates Lung Epithelial Cell Function in Sepsis-Associated ARDS/ALI via LDHA-Mediated NF-κB Signaling. Journal of inflammation research. 2021;14:7035-51.